Journal of Solid Mechanics Vol. 4, No. 2 (2012) pp. 144-158

Electro-Thermo-Mechanical Vibration Analysis of a Foam-Core Smart Composite Cylindrical Shell Containing Fluid

A. Ghorbanpour Arani[1,2*], R. Kolahchi[1]

[1]*Faculty of Mechanical Engineering, University of Kashan, Kashan, Islamic Republic of Iran*
[2]*Institute of Nanoscience & Nanotechnology, University of Kashan, Kashan, Islamic Republic of Iran*

Received 13 February 2012; accepted 16 April 2012

ABSTRACT

In this study, free vibration of a foam-core orthotropic smart composite cylindrical shell (SCCS) filled with a non-viscous compressible fluid, subjected to combined electro-thermo-mechanical loads is investigated. Piezoelectric polymeric cylindrical shell, is made from polyvinylidene fluoride (PVDF) and reinforced by armchair double walled boron nitride nanotubes (DWBNNTs). Characteristics of the equivalent composite are determined using micro-electro-mechanical models. The poly ethylene (PE) foam-core is modeled based on Winkler and Pasternak foundations. Employing the charge equation for coupling electrical and mechanical fields, the problem is turned into an eigenvalue one, for which analytical frequency equations are derived considering free electrical and simply supported mechanical boundary conditions at circular surfaces at either ends of the cylindrical shell. The influence of electric potential generated, filled-fluid, orientation angle of DWBNNTs, foam-core and a few other parameters on the resonance frequency of SCCS are investigated. Results show that SCCS and consequently the generated Φ improve sensor and actuator applications in several process industries, because it not only increases the vibration frequency, but also extends economic viability of the smart structure.

Keywords: DWBNNTs; Smart composite; Fluid-filled cylindrical shell; Foam-core; Free vibration

1 INTRODUCTION

NANO smart composites (NSCs) are materials containing dispersion of nanoparticles in a piezoelectric matrix. Recently, composites with smart nano-reinforcements such as DWBNNTs in piezoelectric polymer like PVDF have been the subject of intense research. In applications where structural integrity is required, NSCs show improved tensile strength, heat deflection temperature, stiffness, and toughness.

Cylindrical shells have vast applications in many engineering fields such as chemical, mechanical aerospace, civil, naval, and nuclear industries. The study of free vibration behavior of circular cylindrical shells has therefore been carried out extensively by many investigators. [1-11]

Fluid-filled cylindrical shells are used in many engineering unit operations and structures, such as pressure vessels, oil tankers, aeroplanes, storage tanks under earthquake waves, nuclear fuel storage poolships, and marine crafts. Junger and Mass [12], and later Jain [13] studied coupled vibrations of fluid-filled cylindrical shells based on shear shell theory and discussed the free vibrations of orthotropic cylindrical shells filled partially or completely with an incompressible, non-viscous fluid. Frequency response of cylindrical shells partially submerged or filled with liquid was investigated by Goncalves and Batista [14]. An exact solution to the free vibration of a transversely

* Corresponding author. Tel.: +98 9131626594 ; Fax: +98 361 55912424.
E-mail address: aghorban@kashanu.ac.ir (A.Ghorbanpour Arani).

isotropic cylindrical shell filled with fluid was proposed by Chen and Ding [15]. Chung [16] compared analytical and experimental investigations carried out by him on the vibration characteristics of cylindrical shells filled with fluid. Amabili [17] studied natural frequencies and mode shapes of a simply-supported circular cylindrical shell, partially filled with liquid and further extended his study to include the free vibrations of these shells entirely filled with a dense fluid and partially immersed in various fluids under different end conditions (Amabili [18]). Pellicano and Amabili [19] studied the stability and vibration of empty and fluid-filled circular cylindrical shells under static and periodic axial loads. Chen et al. [20, 21] improved the previous work by introducing three-dimensional vibration analysis of fluid-filled orthotropic functionally graded piezoelectric cylindrical shells. Later, free vibrations of fluid-filled cylindrical shells on elastic foundations were investigated by Gunawan Tj et al. [22] who studied the effect of fluid and foundation parameters such as spring stiffness on the natural frequency of the shell vibration. Recently, Daneshmand and Ghavanloo [23] investigated the coupled free vibration analysis of a fluid-filled rectangular container with a sagged bottom membrane. Also, coupled vibrations of a partially fluid-filled cylindrical shell was studied by Askari et al. [24] who considered the effect of free surface waves in their analysis.

It is worth noting that none of the articles mentioned above considered NSCs. Vibration analysis of SCCS with great potentials in manufacturing of actuators and sensors slows the transmission of gases and moisture vapor as a consequence of their exceedingly high surface area-to-volume ratio. Regarding composites, Gibson and Ronald [25] studied their numerical behavior when subjected to mechanical and thermal loading. The embedding of piezoelectric materials in the form of fibers into a polymer matrix was implemented by Bent et al [26]. Free vibration of composite plates and cylindrical shell panels were studied by Messina and Soldatos [27] using a higher-order theory. Micro-electro-mechanical models were afterwards used by Tan and Tong [28] to predict the characteristics for piezoelectric-fiber-reinforced composite materials. They investigated effects of geometrical parameters on the effective electroelastic constants, and discussed the convergence of the rectangle-cylinder model. Free vibration and buckling analysis of composite cylindrical shells conveying hot fluid was proposed by Kadoli and Ganesan [29]. Active control of laminated cylindrical shells using piezoelectric fiber reinforced composites was investigated by Ray and Reddy [30]. In another study, vibration and buckling of cross-ply laminated composite circular cylindrical shells were studied by Matsuna [31] based on a global higher-order theory. Rahmani et al. [32] investigated free vibration response of composite sandwich cylindrical shell with flexible core. Buckling and vibration analysis of these plate/shell structures via a smoothed quadrilateral flat shell element with in-plane rotations was studied by Nguyen-Van [33]. Recently, electro-thermo-mechanical torsional buckling of a piezoelectric polymeric cylindrical shell reinforced by DWBNNTs with an elastic core was studied by Mosallaie Barzoki et al. [34].

So far, very few researchers have used charge equation for coupling between electric and mechanical fields, and hence the studies carried out by them mistakenly over-simplify the important influence of electric potential on the resonance frequency. Including this in the analysis presents a complex governing equation with respect to axial, circumferential, longitudinal displacements as well as the electric potential, whose solution can no longer be solved as a normal eigenvalue problem. However, using matrices algebraic rules, the problem is turned into a solvable eigenvalue one. Hence, in this study, effects of the fluid, electric potential and foam-core on the resonance frequency of SCCS, subjected to electro-thermo-mechanical loadings are investigated. Consequently, analytical frequency and electric potentials are derived for free electrical and simply supported mechanical boundary conditions.

2 ELECTROMECHANICAL BEHAVIOUR OF SMART COMPOSITE

Consider a SCCS whose shell is polymeric piezoelectric PVDF as matrix, and is reinforced by armchair DWBNNTs, whose constituents are assumed to be homogeneous. The stresses (mechanical) and electric fields are taken as independent variables in the piezoelectric constitutive equations, and when coupled may be written as [35, 36]

$$\begin{bmatrix}\sigma_{xx}\\ \sigma_{\theta\theta}\\ \sigma_{zz}\\ \tau_{\theta z}\\ \tau_{xz}\\ \tau_{x\theta}\\ D_{xx}\\ D_{\theta\theta}\\ D_{zz}\end{bmatrix}=\begin{bmatrix}C_{11} & C_{12} & C_{13} & 0 & 0 & 0\\ C_{12} & C_{22} & C_{23} & 0 & 0 & 0\\ C_{13} & C_{23} & C_{33} & 0 & 0 & 0\\ 0 & 0 & 0 & C_{44} & 0 & 0\\ 0 & 0 & 0 & 0 & C_{55} & 0\\ 0 & 0 & 0 & 0 & 0 & C_{66}\\ e_{11} & e_{13} & e_{13} & 0 & 0 & 0\\ 0 & 0 & 0 & 0 & 0 & e_{35}\\ 0 & 0 & 0 & 0 & e_{35} & 0\end{bmatrix}\left(\begin{Bmatrix}\overline{\varepsilon_{xx}}\\ \overline{\varepsilon_{\theta\theta}}\\ \overline{\varepsilon_{zz}}\\ 2\overline{\varepsilon_{\theta z}}\\ 2\overline{\varepsilon_{xz}}\\ 2\overline{\varepsilon_{x\theta}}\end{Bmatrix}-\begin{Bmatrix}\alpha_{xx}\\ \alpha_{\theta\theta}\\ \alpha_{zz}\\ 0\\ 0\\ 0\end{Bmatrix}\Delta T\right)-\begin{bmatrix}e_{11} & 0 & 0\\ e_{13} & 0 & 0\\ e_{13} & 0 & 0\\ 0 & 0 & 0\\ 0 & 0 & e_{35}\\ 0 & e_{35} & 0\\ \in_{11} & 0 & 0\\ 0 & \in_{33} & 0\\ 0 & 0 & \in_{33}\end{bmatrix}\begin{Bmatrix}E_{xx}\\ E_{\theta\theta}\\ E_{zz}\end{Bmatrix}, \tag{1}$$

where σ_{ij} and τ_{ij} are the stresses, $\bar{\varepsilon}_{ij}$ is the strain, E_{ii} is the electric field, D_{ii} is the electric displacement and C_{ij}, e_{ij}, $\in_{ii}$ are elastic, piezoelectric, and dielectric constants, while α_{ii} and ΔT refer to thermal expansion coefficient and thermal gradient, respectively. Using approach adopted by Tan and Tong [28] in which they use representative volume element (RVE) base on micro-electro-mechanical models, the mechanical, thermal and electrical properties of the SCCS are determined using Eq. (1) as presented in Appendix A.

3 STRESS - STRAIN RELATIONS

Shear strains $\gamma_{xz}, \gamma_{\theta z}$ are considered negligible in the Kirchhoff deformation theory. Hence, the tangential displacements u, v become linear functions of z, the radial coordinate [37]. In other words

$$\begin{aligned} u(x,\theta,z) &= u(x,\theta) - z\frac{\partial w(x,\theta)}{\partial x}, \\ v(x,\theta,z) &= v(x,\theta) - z\frac{\partial w(x,\theta)}{\partial \theta}, \\ w(x,\theta,z) &= w(x,\theta). \end{aligned} \tag{2}$$

The strain components $\bar{\varepsilon}_{xx}$, $\bar{\varepsilon}_{\theta\theta}$ and $\bar{\gamma}_{x\theta}$ at an arbitrary point of the shell are related to the middle surface strains ε_{xx}, $\varepsilon_{\theta\theta}$ and $\gamma_{x\theta}$ and to the changes in the curvature and torsion of the middle surface k_{xx}, $k_{\theta\theta}$ and $k_{x\theta}$ by the following relationships

$$\begin{Bmatrix} \overline{\varepsilon_{xx}} \\ \overline{\varepsilon_{\theta\theta}} \\ 2\overline{\varepsilon_{x\theta}} \end{Bmatrix} = \begin{Bmatrix} \varepsilon_{xx} \\ \varepsilon_{\theta\theta} \\ \gamma_{x\theta} \end{Bmatrix} - z\begin{Bmatrix} k_{xx} \\ k_{\theta\theta} \\ k_{x\theta} \end{Bmatrix} = \left(\begin{bmatrix} \frac{\partial}{\partial x} & 0 & 0 \\ 0 & \frac{\partial}{R\partial\theta} & \frac{1}{R} \\ \frac{\partial}{2R\partial\theta} & \frac{\partial}{2\partial x} & 0 \end{bmatrix} - z\begin{bmatrix} 0 & 0 & \frac{\partial^2}{\partial x^2} \\ 0 & 0 & \frac{\partial^2}{R^2\partial\theta^2} \\ 0 & 0 & 2\frac{\partial^2 w}{R\partial x\partial\theta} \end{bmatrix} \right) \times \begin{bmatrix} u \\ v \\ w \end{bmatrix}, \tag{3}$$

where u, v and w, describe the displacements in the orthogonal coordinate system x, θ, z, established at the middle surface of the shell .

4 MATHEMATICAL EQUATION OF MOTION FOR SCCS

Fig. 1 illustrates a SCCS filled with fluid, in which l, R_s, h, and ρ_s, correspond to length, mean radius, thickness and density of the shell, respectively. The foam-core has radius R_c, elastic module E_c and Poisson's ratio υ_c.

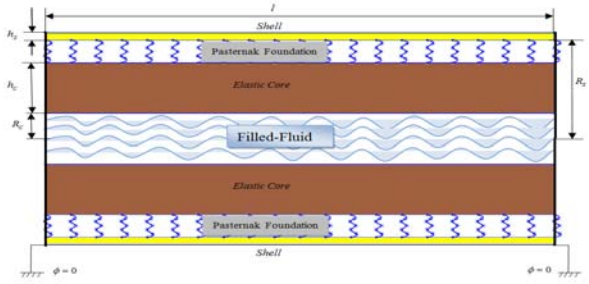

Fig.1
Smart composite cylindrical shell with an elastic core containing fluid.

Charge equation for coupling electrical and mechanical fields is [21]

$$\frac{\partial D_z}{\partial z}+\frac{\partial D_\theta}{R\,\partial\theta}+\frac{\partial D_x}{\partial x}+\frac{D_z}{R}=0, \tag{4}$$

Hence, the three equations of motion for the linear analysis of a cylindrical shell using Donell's shell theory [38] become

$$\begin{aligned}
&\frac{\partial N_{xx}}{\partial x}+\frac{\partial N_{x\theta}}{R\partial\theta}+P_{xx}=\rho h\frac{\partial^2 u}{\partial t^2},\\
&\frac{\partial N_{\theta\theta}}{R\partial\theta}+\frac{\partial N_{x\theta}}{\partial x}+P_{\theta\theta}=\rho h\frac{\partial^2 v}{\partial t^2},\\
&\frac{\partial^2 M_{xx}}{\partial x^2}+\frac{2\partial M_{x\theta}}{R\partial x\partial\theta}+\frac{\partial^2 M_{\theta\theta}}{R^2\partial\theta^2}-\frac{N_{\theta\theta}}{R}+N_{xx}\frac{\partial^2 w}{\partial x^2}+N_{\theta\theta}\frac{\partial^2 w}{R^2\partial\theta^2}+N_{x\theta}\frac{2\partial^2 w}{R\partial x\partial\theta}+P_{zz}=\rho h\frac{\partial^2 w}{\partial t^2},
\end{aligned} \tag{5}$$

where N_{xx}, $N_{\theta\theta}$ and $N_{x\theta}$ express the membrane forces of the middle surface; M_{xx}, $M_{\theta\theta}$ and $M_{x\theta}$ refer to the internal moments; P_{xx}, $P_{\theta\theta}$ and P_{zz} are axial, circumferential and longitudinal external forces; and D_{xx}, $D_{\theta\theta}$ and D_{zz} represent axial, circumferential and longitudinal electric displacements, respectively. At free vibration here, the external forces become zero and since the electrodes are located at either ends of the cylindrical shell with DWBNNTs laid out in the longitudinal direction, $D_{\theta\theta}$ and D_{zz} become zero. D_x on the other hand may be written as [35]:

$$D_{xx}=e_{11}(\varepsilon_{xx}-\alpha_{xx}\Delta T)+e_{13}(\varepsilon_{\theta\theta}-\alpha_{\theta\theta}\Delta T)+\in_{11}E_{xx}, \tag{6}$$

where electric field, E_{xx} , in term of electric potential is [35]:

$$E_{xx}=-\frac{\partial\phi}{\partial x}. \tag{7}$$

Using Eq. (3), the constitute relations expressed in Eq. (1) are reduced to

$$\begin{Bmatrix}\sigma_{xx}\\ \sigma_{\theta\theta}\\ \tau_{x\theta}\\ D_{xx}\end{Bmatrix}=\begin{bmatrix}Q_{11} & Q_{12} & 0 & -e_{11}\\ Q_{12} & Q_{22} & 0 & -e_{13}\\ 0 & 0 & Q_{66} & 0\\ e_{11} & e_{13} & 0 & \in_{11}\end{bmatrix}\begin{Bmatrix}\varepsilon_{xx}-\alpha_{xx}\\ \varepsilon_{\theta\theta}-\alpha_{\theta\theta}\\ \gamma_{x\theta}\\ E_{xx}\end{Bmatrix}, \tag{8}$$

where Q_{ij} is the corresponding elastic constant in global coordinate, defined as:

$$\begin{aligned}
Q_{11}&=C_{11}\cos^4\theta+2(C_{12}+2C_{66})\sin^2\theta\cos^2\theta+C_{22}\sin^4\theta,\\
Q_{12}&=(C_{11}+C_{22}-4C_{66})\sin^2\theta\cos^2\theta+C_{12}(\cos^4\theta+\sin^4\theta),\\
Q_{22}&=C_{11}\sin^4\theta+2(C_{12}+2C_{66})\sin^2\theta\cos^2\theta+2C_{22}\cos^4\theta,\\
Q_{66}&=(C_{11}+C_{22}-2C_{12}-2C_{66})\sin^2\theta\cos^2\theta+C_{66}(\sin^4\theta+\cos^4\theta).
\end{aligned} \tag{9}$$

Here, θ is the orientation angle between the global and local cylindrical co-ordinates, corresponding to the angle between DWBNNTs and the main axis of the matrix.

Integrating the stresses and the remaining electric displacement across the thickness of shell yields

$$\begin{Bmatrix} N_{xx} \\ N_{\theta\theta} \\ N_{x\theta} \\ G_{xx} \end{Bmatrix} = \int_{-\frac{h}{2}}^{\frac{h}{2}} \begin{Bmatrix} \sigma_{xx} \\ \sigma_{\theta\theta} \\ \tau_{x\theta} \\ D_{xx} \end{Bmatrix} \mathrm{d}z = \begin{bmatrix} A_{11} & A_{12} & 0 & P_{11} \\ A_{12} & A_{22} & 0 & P_{12} \\ 0 & 0 & A_{66} & 0 \\ P_{11} & P_{12} & 0 & Y_{11} \end{bmatrix} \begin{Bmatrix} \varepsilon_{xx} \\ \varepsilon_{\theta\theta} \\ \gamma_{x\theta} \\ E_{xx} \end{Bmatrix} - \begin{bmatrix} B_{11} & B_{12} & 0 & F_{11} \\ B_{12} & B_{22} & 0 & F_{12} \\ 0 & 0 & B_{66} & 0 \\ F_{11} & F_{12} & 0 & 0 \end{bmatrix} \begin{Bmatrix} k_{xx} \\ k_{\theta\theta} \\ k_{x\theta} \\ E_{xx} \end{Bmatrix} - \begin{bmatrix} N_{xx}^{T} \\ N_{\theta\theta}^{T} \\ 0 \\ 0 \end{bmatrix}, \tag{10}$$

$$\begin{Bmatrix} M_{xx} \\ M_{\theta\theta} \\ M_{x\theta} \\ Q_{xx} \end{Bmatrix} = \int_{-\frac{h}{2}}^{\frac{h}{2}} \begin{Bmatrix} \sigma_{xx} \\ \sigma_{\theta\theta} \\ \tau_{x\theta} \\ D_{xx} \end{Bmatrix} z\,\mathrm{d}z = \begin{bmatrix} B_{11} & B_{12} & 0 & F_{11} \\ B_{12} & B_{22} & 0 & F_{12} \\ 0 & 0 & B_{66} & 0 \\ F_{11} & F_{12} & 0 & H_{11} \end{bmatrix} \begin{Bmatrix} \varepsilon_{xx} \\ \varepsilon_{\theta\theta} \\ \gamma_{x\theta} \\ E_{xx} \end{Bmatrix} - \begin{bmatrix} S_{11} & S_{12} & 0 & J_{11} \\ S_{12} & S_{22} & 0 & J_{12} \\ 0 & 0 & S_{66} & 0 \\ J_{11} & J_{12} & 0 & 0 \end{bmatrix} \begin{Bmatrix} k_{xx} \\ k_{\theta\theta} \\ k_{x\theta} \\ E_{xx} \end{Bmatrix} - \begin{bmatrix} M_{xx}^{T} \\ M_{\theta\theta}^{T} \\ 0 \\ 0 \end{bmatrix}, \tag{11}$$

where

$$\begin{pmatrix} \{A_{ij},\ B_{ij},\ S_{ij}\} \\ \{P_{ij},\ F_{ij},\ J_{ij}\} \\ \{Y_{ij},\ H_{ij},\ 0\} \\ \{N_{nn}^{T},\ M_{nn}^{T},\ 0\} \end{pmatrix} = \int_{-\frac{h}{2}}^{\frac{h}{2}} \begin{pmatrix} \{1,\ z,\ z^2\} \\ \{1,\ z,\ z^2\} \\ \{1,\ z,\ 0\} \\ \{1,\ z,\ 0\} \end{pmatrix} \times \begin{pmatrix} \{C_{ij}\} \\ \{-e_{ij}\} \\ \{-\in_{ii}\} \\ \{\alpha_{nn}C_{ij}\} \end{pmatrix} \mathrm{d}z \qquad [i,j=1,2,...6] \quad [n=x,\theta]. \tag{12}$$

4.1 Boundary conditions

As mentioned before, in the free vibrations of a SCCS, the boundary conditions defined for two ends circular surfaces are free electrical and simply supported mechanical boundary conditions. For the electrical boundary conditions, $\phi=0$, and for the mechanical one $u=v=w=w_{,xx}=0$.The mechanical boundary condition is selected because in practice simply supported ends could be achieved approximately by connecting the shell to thin end plates and rings. Hence, the three displacement and one electric potential mode shapes may be written as [21]:

$$\mathbf{d} = \begin{Bmatrix} u \\ v \\ w \\ \phi \end{Bmatrix} = \begin{Bmatrix} A_1 \cos(\frac{m\pi x}{l}) \cos(n\theta) \cos(\omega t) \\ A_2 \sin(\frac{m\pi x}{l}) \sin(n\theta) \cos(\omega t) \\ A_3 \sin(\frac{m\pi x}{l}) \cos(n\theta) \cos(\omega t) \\ A_4 \cos(\frac{m\pi x}{l}) \cos(n\theta) \cos(\omega t) \end{Bmatrix}, \tag{13}$$

where ω represents vibration frequency of shell, m and n are half axial and circumferential wave numbers, respectively. It should be noted that m is any positive number, while n is an integer, and $A_i, (i=1,..,4)$ represent displacement and electric potential amplitudes.

4.2 Solution procedure

To generalize the solution, all variables are made dimensionless. For this, the following dimensionless quantities are introduced

$$\bar{A}_i = \frac{A_i}{h}, (i = 1, ..., 3), \bar{A}_4 = \frac{A_4}{h\Phi_0}, \beta = \frac{h}{R_s}, \chi = \frac{l}{R_s}, \bar{C}_{12} = \frac{C_{12}}{C_{11}}, \bar{C}_{22} = \frac{C_{22}}{C_{11}}, \bar{C}_{66} = \frac{C_{66}}{C_{11}}, \bar{e}_{11} = \frac{e_{11}}{\sqrt{C_{11} \in_{11}}},$$
$$\bar{e}_{13} = \frac{e_{13}}{\sqrt{C_{11} \in_{11}}}, \bar{E}_c = \frac{E_c}{C_{11}}, \Phi_0 = \sqrt{\frac{C_{11}}{\in_{11}}}, \Gamma_1 = \frac{e_{11}\Phi_0}{C_{11}}, \Gamma_2 = \frac{e_{11}}{\in_{11} \Phi_0}, \Gamma_3 = \frac{e_{13}}{\in_{11} \Phi_0}, \bar{t} = \frac{t}{l}\sqrt{\frac{C_{11}}{\rho_s}}. \quad (14)$$

4.2.1 Fluid structure

For a hollow cylinder completely filled with compressible, non-viscous fluid, the mechanical force can be written as [21]:

$$P_f = \frac{-\Omega^2 q_f \overline{w} \rho_f}{\rho_s}, \quad (15)$$

where q_f is

$$q_f = \begin{cases} \dfrac{2J_n(v)}{(J_{n-1}(v) - J_{n+1}(v))v} & v^2 > 0 \\ \dfrac{1}{n}, & v^2 = 0 \\ \dfrac{2I_n(\tilde{v})}{(I_{n-1}(\tilde{v}) + I_{n+1}(\tilde{v}))\tilde{v}} & v^2 = -\tilde{v}^2 < 0 \end{cases}, \quad (16)$$

where ρ_f is the density of fluid and therefore $\rho_f = 0$, corresponds to a case where no fluid is present. Also, $J_n(v)$ and $I_n(v)$ are Bessel and modified Bessel functions of the first kind, respectively. v is on the other hand a dimensionless parameter defined as :

$$v^2 = V^2 \Omega^2 - (m\pi / \chi)^2, \quad (17)$$

where $V = c_s / c_f$, in which c_f is the sound velocity in fluid and $c_s = \sqrt{C_{11}/\rho_s}$ is the velocity of elastic wave in the solid and $\Omega = h\omega\sqrt{\frac{\rho_s}{C_{11}}}$ is dimensionless frequency.

4.2.2 Foam core structure

In this study, the elastic foam core, made from PE is modelled as the Winkler spring constant and the Pasternak shear constant for the SCCS. The foam core force applied to the SCCS is then expressed as [38]:

$$F_o = P_o(2\pi R_s) = (K_w w - K_G \nabla^2 w), \quad (18)$$

where K_w and K_G are Winkler and Pasternak modules, respectively, and P_o is also the pressure generated on the foam core outer interface due to shell vibration. Based on the assumption of a linear, homogeneous and isotropic foam core the pressure P_o may be written as [39]:

$$P_o = \frac{E_c w}{R_c(1-\upsilon_c)} \frac{1-\eta^2}{1+\eta^2}, \quad (19)$$

where in-fill ratio η (corresponding to the thickness of the foam core) is also defined as $\eta = R_c/R_s$. Replacing the boundary condition in z direction, w, in Eq. (18), yields the foam-core force as:

$$\overline{F}_o = \frac{2\pi \overline{E}_c}{1-\upsilon_c}\frac{1-\eta^2}{1+\eta^2}. \tag{20}$$

4.2.3 Overall governing equations

In order to obtain the expressions for forces and moments of the shell, the surface strains and curvatures in Eq. (3) are substituted into Eqs. (6-11). Replacing these into the shell dynamic Eq. (5) and charge Eq. (4), the overall governing equations for a modified SCCS in which fluid and foam-core forces are taken into account, may be written in the differential operator form as:

$$\left(\mathbf{L} - \Omega^2 \mathbf{M}\right)\mathbf{D} = \mathbf{0} \tag{21}$$

where $\mathbf{M}_{4\times4}$, $\mathbf{D}_{4\times1}$ and $\mathbf{L}_{4\times4}$ are defined as:

$$\mathrm{M} = \begin{bmatrix} \beta^2/\chi^2 & 0 & 0 & 0 \\ 0 & \beta^2/\chi^2 & 0 & 0 \\ 0 & 0 & \beta^2/\chi^2 + q_f & 0 \\ 0 & 0 & 0 & 0 \end{bmatrix}, \mathrm{D} = \begin{bmatrix} \overline{A}_1 \\ \overline{A}_2 \\ \overline{A}_3 \\ \overline{A}_4 \end{bmatrix} \tag{22}$$

$$\mathrm{L} = \begin{bmatrix} \frac{-\beta^2 m^2\pi^2}{\chi^2} - \beta^2\overline{C}_{66}n^2 & \frac{\beta^2\overline{C}_{12}m\pi n}{\chi} + \frac{\beta^2\overline{C}_{66}n\pi m}{\chi} & \frac{\beta^2\overline{C}_{12}m\pi}{\chi} & \frac{-\beta^2\Gamma_1 m^2\pi^2}{\chi^2} \\ \frac{\beta^2\overline{C}_{12}m\pi n}{\chi} + \frac{\beta^2\overline{C}_{66}n\pi m}{\chi} & \frac{-\beta^2\overline{C}_{66}m^2\pi^2}{\chi^2} - \beta^2\overline{C}_{22}n^2 & -\beta^2\overline{C}_{22}n & \frac{\beta^2 m\pi n\Gamma_3}{\chi} \\ \frac{\beta^2\overline{C}_{12}m\pi}{\chi} & -\beta^2\overline{C}_{22}n & \overline{\Psi} + \overline{F}_0 & -\frac{\beta^2 m\pi\Gamma_3}{\chi} \\ \frac{-\beta^2\Gamma_2 m^2\pi^2}{\chi^2} & \frac{\beta^2\Gamma_3 m\pi n}{\chi} & \frac{\beta^2\Gamma_3 m\pi}{\chi} & \frac{\beta^2 m^2\pi^2}{\chi^2} \end{bmatrix}, \tag{23}$$

and

$$\overline{\Psi} = \frac{-\beta^4\Gamma_2 m^4\pi^4}{12\chi^4} - \frac{\beta^4\overline{C}_{12}m^2\pi^2n^2}{6\chi^2} - \frac{\beta^4\overline{C}_{66}m^2\pi^2n^2}{3\chi^2} - \beta^4\overline{C}_{22}n^4 - (\alpha_x + \overline{C}_{12}\alpha_\theta)\Delta T\frac{\beta^2m^2\pi^2}{\chi^2} - \beta^2\overline{C}_{22}. \tag{24}$$

However, as can be seen from Eq. (22), in the ($\mathbf{M}_{4\times4}$) matrix, there are both a row and a column with zero arrays, making the problem unsolvable using eigenvalue technique. Applying algebraic rules for matrices, could assist in omitting these zero arrays and turning the governing equation into the following linear relation, which can now be solved using the eigenvalue technique.

$$\left(\begin{bmatrix} L_{11} & L_{12} & L_{13} \\ L_{21} & L_{22} & L_{23} \\ L_{31} & L_{32} & L_{33} \end{bmatrix} - \begin{bmatrix} L_{14} \\ L_{24} \\ L_{34} \end{bmatrix} \begin{bmatrix} L_{44} \end{bmatrix}^{-1} \begin{bmatrix} L_{41} & L_{42} & L_{43} \end{bmatrix} - \Omega^2 \begin{bmatrix} M_{11} & 0 & 0 \\ 0 & M_{22} & 0 \\ 0 & 0 & M_{33} \end{bmatrix} \right) \begin{bmatrix} \overline{A}_1 \\ \overline{A}_2 \\ \overline{A}_3 \end{bmatrix} = 0. \tag{25}$$

Let the matrix determinant be zero to obtain the non-dimensional frequency Ω. Replacing Ω in Eq. (25) yields the displacement amplitudes A_1, A_2 and A_3. However, the electric amplitude may be expressed as:

$$[\overline{A}_4] = [L_{44}]^{-1}[L_{41} \quad L_{42} \quad L_{43}]\begin{bmatrix}\overline{A}_1\\ \overline{A}_2\\ \overline{A}_3\end{bmatrix}. \tag{26}$$

The amplitude ratios of the vibration modes associated with Eq. (25) becomes

$$\begin{bmatrix}\frac{\overline{A}_1}{\overline{A}_3}\\ \frac{\overline{A}_2}{\overline{A}_3}\end{bmatrix} = \left(\begin{bmatrix}L_{11} & L_{12}\\ L_{21} & L_{22}\end{bmatrix} - \begin{bmatrix}\frac{L_{14}L_{41}}{L_{44}} & \frac{L_{14}L_{42}}{L_{44}}\\ \frac{L_{24}L_{41}}{L_{44}} & \frac{L_{24}L_{42}}{L_{44}}\end{bmatrix}\right)^{-1}\begin{bmatrix}L_{13}-\frac{L_{14}L_{43}}{L_{44}}\\ L_{23}-\frac{L_{24}L_{43}}{L_{44}}\end{bmatrix}. \tag{27}$$

In Eq. (27), the ratios $\overline{A}_1/\overline{A}_3$ and $\overline{A}_2/\overline{A}_3$ describe the amplitude ratios. In the above, A_3, the remaining third coefficient in Eq. (25), is treated as a scale factor representing the vibration amplitude.

5 RESULT AND DISCUSSION

Assuming water is the filling fluid, its effects ($\rho_f = 1000$ Kg/m^3), as well as those of the partially filled foam-core and electric potential on the dimensionless resonant frequencies (Ω) and the associated dimensionless amplitude ratios ($\overline{A}_1/\overline{A}_3$ and $\overline{A}_2/\overline{A}_3$) of simply supported SCCS with $R_s = 20$ cm , $l = 100$ cm , $h_s = 0.03$ cm can now be investigated using the proposed method. The material properties of SCCS with PVDF as a matrix were found to be as follows [34]:

$$C_{11} = 238.24 \text{ Gpa}, C_{22} = 23.6 \text{ GPa}, C_{12} = 3.98 \text{ GPa}, C_{66} = 6.43 \text{ GPa}, e_{11} = -0.135 \text{ C/m}^2,$$
$$e_{12} = -0.145 \text{ C/m}^2, \alpha_x = 7.1e-5 \text{ 1/K}, \alpha_\theta = 7.1e-5 \text{ 1/K}.$$

Employing DWBNNTs as the matrix reinforcer provides the following material properties [34]:

$$E = 1.8 \text{ Tpa}, \upsilon = 0.34, e_{11} = 0.95 \text{ C/m}^2, \alpha_x = 1.2e-6 \text{ 1/K}, \alpha_\theta = 0.6e-6 \text{ 1/K}.$$

For PE foam-core, the material properties are [34]:

$$E_c = 125 \text{ Gpa}, \upsilon_c = 0.30.$$

In the present work, the vibration of SCCS with an elastic core containing fluid has been studied. Since, no reference to such a work is found to-date in the literature, its validation is not possible. However, in an attempt to validate this work as far as possible, axial buckling of SCCS with an elastic core was studied which in the absence of electric field and fluid and considering $\rho = 0$, $E_s = 200$GPa , $\upsilon_s = 0.3$, $h = 0.1524$mm , $R_s = 76.2$mm , $L_s = 100$mm and $\upsilon_f = 0.1$ is similar to that presented by [11]. For this purpose, the displacement satisfying our boundary condition is [11]:

$$w = q.\sin\left[\pi\left(\alpha - \frac{x}{L}\right)\right]\sin\left[\pi\left(\frac{x}{L} - 1\right)\right], \tag{28}$$

where q and α are amplitude and circumferential wave number, respectively. At this stage, shell critical stress (σ_x^{crit}) is determined by dividing N_x^{crit} to the thickness of shell (h). (σ_x^{crit}) is then normalized, by dividing it to σ_0 defined as:

$$\sigma_0 = \frac{1}{\sqrt{3}} \cdot \frac{E_s}{\sqrt{1-\nu^2}} \left(\frac{h}{R_s} \right). \tag{29}$$

Fig. 2 illustrates the results of validation exercise by plotting $\sigma_x^{crit} / \sigma_0$ versus η for $E_c / E_s = 10^{-1}$ in the presence and absence of electric field. As can be seen, in case of no electric field, the results obtained are the same as those expressed in [11], indicating validation of our work.

Fig. 3 illustrates the graph of dimensionless frequency Ω, versus circumferential wave number, *n*, for different half axial wave number, *m*, in both fluid-filled and empty shells. As can be seen, Ω is lower for fluid-filled than the empty shell, and the higher the *m*, the higher is the Ω. The influence of fluid on the vibration frequency is so significant that it matches for *m*=1 in empty shell with that of *m*=17 for a similar shell filled with fluid. When shell is filled with the fluid, Ω does not vary significantly as *m* increases, while for empty shells, Ω increases with increase in *m*.

Fig. 4 shows the dimensionless frequency Ω versus orientation angle θ of DWBNNT in the polymer, at various sound speeds, *V*. This is a periodic function with a period of 2π, indicating that higher sound speed in the fluid causes the vibration frequency to be raised. The change in frequency is much more significant for low sound speed in the fluid, *V*, than higher ones. The observation that there is little changes in frequency for higher sound speed, matches that of reference [21].

Fig. 5 demonstrates Ω against ratio of infill, η, for different stiffness ratios of (E_c/E_s) without considering the charge equation which shows effect of electric potential, Φ generated due to piezoelectric characteristics of the SCCS. Fig. 6 is the same as Fig. 5, however the effect of electric potential is considered in it. These figures show that in general, the electric potential increases vibration frequency, and also as η increased (or form-core percentage is reduced), the frequency Ω decreases and this decrease appear to be more significant at higher η's. The stiffer the foam-core, the higher is the vibration frequency and the higher is the variation in Ω. In the absence of Φ as in Fig. 4, little change in Ω is observed up to η=0.3 which makes foam-cores with η higher than o.3 not economically justifiable. However, presence of Φ (as in Fig. 6) extends this limit of η=o.3 to 0.65. This result illustrates the economic importance of applying smart composite in this work, since Φ generated along the cylindrical shell not only increase Ω but also reduces the need for the foam-core to bring down the magnitude of Ω.

As regards the geometric characteristics, Fig. 7 shows the graph of Ω versus the aspect ratio (R_s/h) for different η's, indicating a sharp decrease in Ω within the aspect ratio range of 20-40, above which Ω reduces very slightly. This trend is observed irrespective of the η applied.

To highlight the importance of the influence of generated electric field being investigated in this study, Fig. 8 is produced to present variation in Φ generated due to piezoelectric characteristics of the SCCS along the cylinder length for various η. As can be seen from Fig. 8 (plotted for *m*=2 and *n*=1), the higher the η's, the higher is the amplitude of Φ generated, and consequently the lower is the Ω. It is also concluded that the free electrical boundary conditions is satisfied in the circular surfaces at both ends of the SCCS.

Fig. 9 shows the variations of Φ generated against time for different η's, indicating a period of 12 seconds irrespective of η's used. In the solid foam-core (i.e. η=0), the amplitude of Φ generated remains small (up to 0.1), but as η is increased, it increases to a maximum of 2.2.

Graphs of amplitude ratios $\overline{A}_1/\overline{A}_3$ and $\overline{A}_2/\overline{A}_3$ against *m* for different values of *n* are plotted in Figs. 10 and 11, respectively. As the half axial wave number *m* is increased from 1 to 10, the dimensionless amplitude ratio is reduced and finally converges to a fix value as *n* is increased.

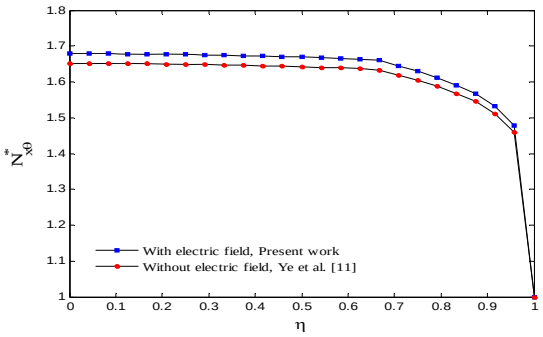

Fig.2
Dimensionless critical stress versus η for $E_c / E_s = 10^{-1}$ in the presence and absence of electric field.

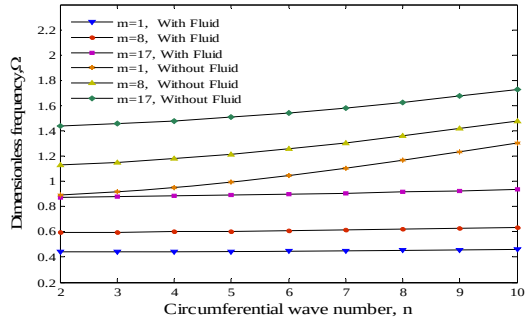

Fig.3
Dimensionless frequency versus circumferential wave number for different half axial wave numbers for both fluid-filled and empty shell.

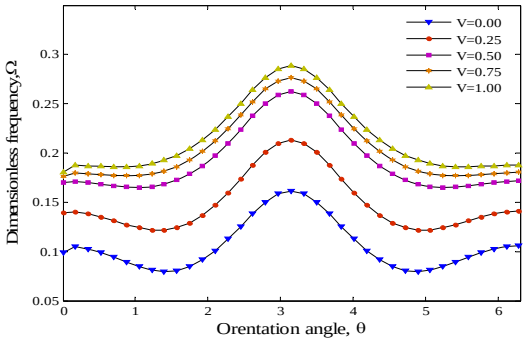

Fig.4
Dimensionless frequency versus orientation angle of DWBNNT at various sound speeds.

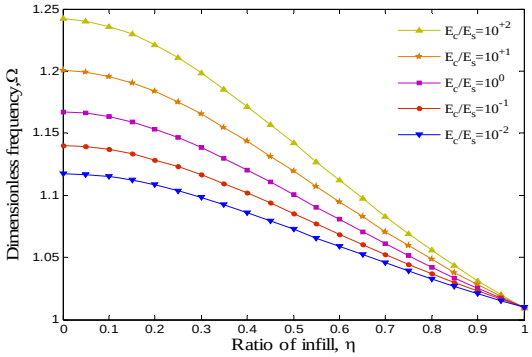

Fig.5
Dimensionless frequency versus ratio of infill for different stiffness ratios of foam-core without considering electric potential.

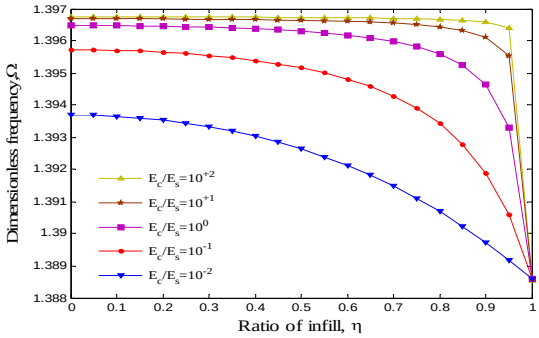

Fig.6
Dimensionless frequency versus ratio of infill for different stiffness ratios of foam-core with considering electric potential.

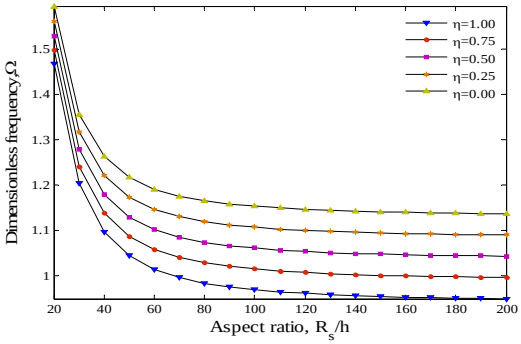

Fig.7
Dimensionless frequency versus the aspect ratio for different ratios of infill.

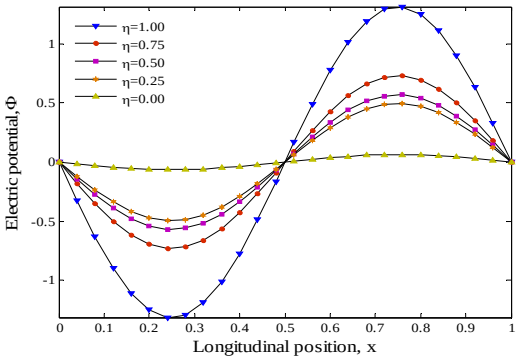

Fig.8
Electric potential versus the cylinder length for different ratios of infill.

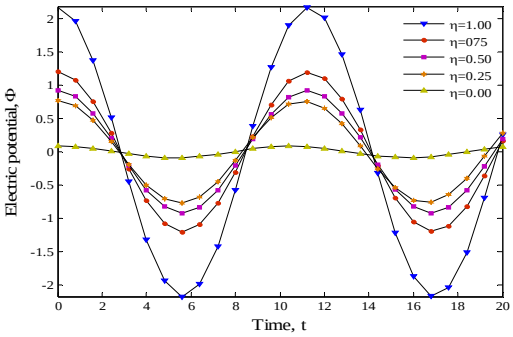

Fig.9
Electric potential versus time for different ratios of infill.

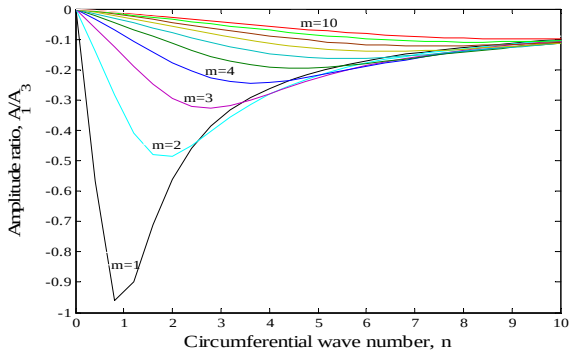

Fig.10
Amplitude ratio $\overline{A}_1/\overline{A}_3$ versus circumferential wave number for different values of half axial wave numbers.

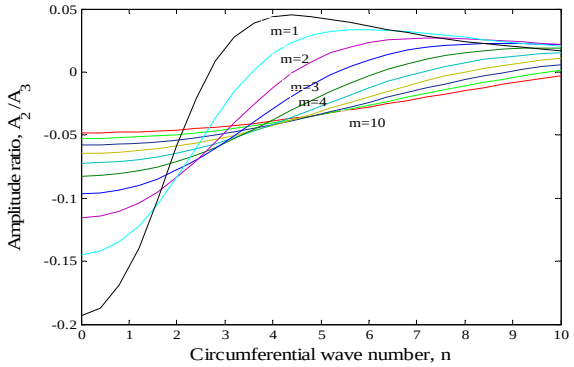

Fig.11
Amplitude ratio $\overline{A}_2/\overline{A}_3$ versus circumferential wave number for different values of half axial wave numbers.

6 CONCLUSION

Applying charge equation for coupling mechanical and electrical fields, the influence of electric potential generated due to piezoelectric characteristics Φ, filled-fluid and foam-core were investigated on the resonance frequency Ω of a smart composite cylindrical shell, SCCS, made from PVDF matrix reinforced with DWBNNTs having a PE foam-core filled with a fluid. Electric potential increases the resonance frequency considerably, indicating a favourite potential for this smart structure to be used in actuators and sensors in a range of industrial applications.

Following investigating the orientation angle of reinforced nanotube, geometrical characteristics of the structure and the stiffness ratio of the foam-core, it could be said that increasing in-fill ratio of the foam-core η, decreased Ω. Application of SCCS and consequently the generated Φ, extend economic viability of the smart structure from in-fill ratio η=o.3 to η=0.65, thereby reducing the need for the foam-core to bring down the magnitude of Ω. Also, Ω is lower for fluid-filled than the empty shell and the influence of filled fluid on the vibration frequency is so significant that the Ω matches for m=1 in empty shell with that of m=17 for a similar shell filled with fluid.

ACKNOWLEDGMENTS

The authors are grateful to University of Kashan for supporting this work by Grant No. 65475/35 This research was supported by the Thermoelasticity Center of Excellence, Mechanical Engineering Department, Amirkabir University of Technology.

APPENDIX A

$$
\begin{aligned}
&C_{11}=\frac{C_{11}^{r}C_{11}^{m}}{\rho C_{11}^{m}+(1-\rho)C_{11}^{r}},\\
&C_{12}=C_{11}\left[\frac{\rho C_{12}^{r}}{C_{11}^{r}}+\frac{+(1-\rho)C_{12}^{m}}{C_{11}^{m}}\right],\\
&C_{13}=C_{11}\left[\frac{\rho C_{13}^{r}}{C_{11}^{r}}+\frac{+(1-\rho)C_{13}^{m}}{C_{11}^{m}}\right],\\
&C_{22}=\rho C_{22}^{r}+(1-\rho)C_{22}^{m}+\frac{C_{12}^{2}}{C_{11}}-\frac{\rho(C_{12}^{r})^{2}}{C_{11}^{r}}-\frac{(1-\rho)(C_{12}^{m})^{2}}{C_{11}^{m}},\\
&C_{23}=\rho C_{23}^{r}+(1-\rho)C_{23}^{m}+\frac{C_{12}C_{13}}{C_{11}}-\frac{\rho C_{12}^{r}C_{13}^{r}}{C_{11}^{r}}-\frac{(1-\rho)C_{12}^{m}C_{13}^{m}}{C_{11}^{m}},\\
&C_{44}=\rho C_{44}^{r}+(1-\rho)C_{44}^{m},\\
&C_{55}=\frac{A}{B^{2}+AC},\\
&C_{66}=\frac{C_{66}^{r}C_{66}^{m}}{\rho C_{66}^{m}+(1-\rho)C_{66}^{r}},\\
&e_{31}=C_{11}\left[\frac{\rho e_{31}^{r}}{C_{11}^{r}}+\frac{+(1-\rho)e_{31}^{m}}{C_{11}^{m}}\right],\\
&e_{32}=\rho e_{32}^{r}+(1-\rho)e_{32}^{m}+\frac{C_{12}e_{31}}{C_{11}}-\frac{\rho C_{12}^{r}e_{31}^{r}}{C_{11}^{r}}-\frac{(1-\rho)C_{12}^{m}e_{31}^{m}}{C_{11}^{m}},\\
&e_{33}=\rho e_{33}^{r}+(1-\rho)e_{33}^{m}+\frac{C_{13}e_{31}}{C_{11}}-\frac{\rho C_{13}^{r}e_{31}^{r}}{C_{11}^{r}}-\frac{(1-\rho)C_{13}^{m}e_{31}^{m}}{C_{11}^{m}},\\
&e_{24}=\rho e_{24}^{r}+(1-\rho)e_{24}^{m},\\
&e_{15}=\frac{B}{B^{2}+AC},\\
&\in_{11}=\frac{C}{B^{2}+AC},\\
&\in_{22}=\rho\in_{22}^{r}+(1-\rho)\in_{22}^{m},\\
&\in_{33}=\rho\in_{33}^{r}+(1-\rho)\in_{33}^{m}-\frac{e_{31}^{2}}{C_{11}}+\frac{\rho(e_{31}^{r})^{2}}{C_{11}^{r}}+\frac{(1-\rho)(e_{31}^{m})^{2}}{C_{11}^{m}},
\end{aligned}
\tag{A.1}
$$

where

$$
\begin{aligned}
&A=\frac{\rho C_{55}^{r}}{(e_{15}^{r})^{2}+C_{55}^{r}\in_{11}^{r}}+\frac{(1-\rho)C_{55}^{m}}{(e_{15}^{m})^{2}+C_{55}^{m}\in_{11}^{m}},\ B=\frac{\rho e_{15}^{r}}{(e_{15}^{r})^{2}+C_{55}^{r}\in_{11}^{r}}+\frac{(1-\rho)e_{15}^{m}}{(e_{15}^{m})^{2}+C_{55}^{m}\in_{11}^{m}},\\
&C=\frac{\rho\in_{11}^{r}}{(e_{15}^{r})^{2}+C_{55}^{r}\in_{11}^{r}}+\frac{(1-\rho)\in_{11}^{m}}{(e_{15}^{m})^{2}+C_{55}^{m}\in_{11}^{m}},
\end{aligned}
\tag{A.2}
$$

Subscripts r and m refer to the reinforced and matrix components of the composite, respectively. ρ is also the vol % of the reinforced DBNNTs.

REFERENCES

[1] Love A.E.H., 1888, On the small free vibrations and deformations of a thin elastic shell, *Philosophical Transactions of the Royal Society* A **179**: 491–549.

[2] Arnold R.N., Warburton G.B., 1948, Flexural vibrations of the walls of thin cylindrical shells, *Philosophical Transactions of the Royal Society* **197**: 238-256.

[3] Bert C.W., Baker J.L., Egle B.M., 1969, Free vibration of multilayer anisotropic cylindrical shells, *Journal of Composite Material* **3**: 480-499.

[4] Blevins R.D., 1979, *Formulas for Natural Frequency and Mode Shape*, Van Nostrand Reinhold, New York.

[5] Soedel W.A., 1980, New frequency formula for closed circular cylindrical shells for a large variety of boundary conditions, *Journal of Sound and Vibration* **70**: 309-317.

[6] Vanderpool M.E., Bert C.W., 1981, Vibration of materially monoclinic thick-wall circular cylindrical shell, *American Institute of Aeronautics and Astronautics* **19**: 634-641 .

[7] Ludwig A., Krieg R., 1981, An analysis quasi-exact method for calculating eigen vibrations of thin circular shells, *Journal of Sound and Vibration* **74**: 155-174.

[8] Chung H., Turul P., Mulcahy T.M., Jendrzejczyk J.A., 1981, Analysis of a cylindrical shell vibrating in a cylindrical fluid region, *Nuclear Engineering Design* **63**: 109–120.

[9] Markus S., 1988, *The Mechanics of Vibrations of Cylindrical Shells*, Elsevier, New York.

[10] Xianga Y., Mab Y.F., Kitipornchaib S., Lim C.W., Lau C.W.H., 2002, Exact solutions for vibration of cylindrical shells with intermediate ring supports, *International Journal of Mechanical Science* **44**: 1907–1924.

[11] Ye L., Lun G., Ong L.S., 2011, Buckling of a thin-walled cylindrical shell with foam core under axial compression, *Thin-Walled Struct* **49**: 106–111.

[12] Junger M.C., Mass C., 1952, Vibration of elastic shells in a fluid medium and the associated radiation of sound, *Journal of Applied Mechanics* **74**: 439–445.

[13] Jain R.K., 1974, Vibration of fluid-filled orthotropic cylindrical shells, *Journal of Sound and Vibration* **37**: 379–388.

[14] Goncalves P.B., Batista R.C., 1987, Frequency response of cylindrical shells partially submerged or filled with liquid, *Journal of Sound and Vibration* **113**: 59–70.

[15] Chen W.Q., Ding H.J., 1999, Natural frequencies of fluid-filled transversely isotropic cylindrical shells, *International Journal of Mechanical Science* **41**: 677–684.

[16] Chung H., 1981, Free vibration analysis of circular cylindrical shells, *Journal of Sound and Vibration* **74**: 331-359.

[17] Amabili M. 1999, Vibrations of circular tubes and shells filled and partially immersed in dense fluids, *Journal of Sound and Vibration* **221**: 567–585.

[18] Amabili M., 1996, Free vibration of partially filled horizontal cylindrical shells, *Journal of Sound and Vibration* **191**: 757–780.

[19] Pellicano F., Amabili M., 2003, Stability and vibration of empty and fluid-filled circular cylindrical shells under static and periodic axial loads, *International Journal of Solids and Structures* **40**: 3229–3251.

[20] Chen W.Q., Bian Z.G., Ding H.J., 2004, Three-dimensional vibration analysis of fluid-filled orthotropic FGM cylindrical shells, *International Journal of Mechanical Science* **46**: 159–171.

[21] Chen W.Q., Bian Z.G., Lv C.F., Ding H.J. 2004, 3D free vibration analysis of a functionally graded piezoelectric hollow cylinder filled with compressible fluid International, *International Journal of Solids and Structures* **41**: 947–964.

[22] Tj H.G., Mikami T., Kanie S., Sato M., 2005, Free vibrations of fluid-filled cylindrical shells on elastic foundations, *Thin-Wall Structures* **43**: 1746–1762.

[23] Daneshmand F., Ghavanloo E., 2010, Coupled free vibration analysis of a fluid-filled rectangular container with a sagged bottom membrane, *Journal of Fluids and Structures* **26**: 236–252.

[24] Askari E., Daneshmand F., Amabili M., 2011, Coupled vibrations of a partially fluid-filled cylindrical container with an internal body including the effect of free surface waves, *Journal of Fluids and Structures* **27**: 1049–1067.

[25] Gibson K., Ronald F.,1994, *Principles of Composite Material Mechanics*, McGraw Hill, New York.

[26] Bent A.A., Hagood N.W., Rodgers J.P., 1995, Anisotropic actuation with piezoelectric fiber composites, *Journal of Material System Structures* **6**: 338–349.

[27] Messina A., Soldatos K.P., 1999, Vibration of completely free composite plates and cylindrical shell panels by a higher-order theory, *International Journal of Mechanical Science* **41**: 891-918.

[28] Tan P., Tong L., 2001, Micro-electromechanics models for piezoelectric-fiber-reinforced composite materials, *Composite Science Technology* **61**: 759–769.

[29] Kadoli R., Ganesan N., 2003, Free vibration and buckling analysis of composite cylindrical shells conveying hot fluid, *Composite Structures* **60**: 19–32.

[30] Ray M.C., Reddy J.N., 2005, Active control of laminated cylindrical shells using piezoelectric fiber reinforced composites, *Composite Science Technology* **65**: 1226–1236.

[31] Matsuna H., 2007, Vibration and buckling of cross-ply laminated composite circular cylindrical shells according to a global higher-order theory, *International Journal of Mechanical Science* **49**: 1060-1075.

[32] Rahmani O., Khalili S.M.R., Malekzadeh K., 2010, Free vibration response of composite sandwich cylindrical shell with flexible core, *Composite Structures* **92**: 1269–1281.

[33] Nguyen-Van H., Mai-Duy N., Karunasena W., Tran-Cong T., 2011, Buckling and vibration analysis of laminated composite plate/shell structures via a smoothed quadrilateral flat shell element with in-plane rotations, *Computers and Structures* **89**: 612–625.

[34] Mosallaie Barzoki A.A., Ghorbanpour Arani A., Kolahchi R., Mozdianfard M.R., 2011, Electro-thermo-mechanical torsional buckling of a piezoelectric polymeric cylindrical shell reinforced by DWBNNTs with an elastic core, *Applied Mathematical Modelling* **27**: 1278-1284.

[35] Ghorbanpour Arani A., Kolahchi R., Mosallaie Barzoki A.A., 2011, Effect of material inhomogeneity on electro-thermo-mechanical behaviors of functionally graded piezoelectric rotating cylinder, *Applied Mathematical Modelling* **35**: 2771–2789.

[36] Ghorbanpour Arani A., Kolahchi R., Mosalaei Barzoki A.A., Loghman A., 2012, Electro-thermo-mechanical behaviors of FGPM Spheres Using Analytical Method and ANSYS Software, *Applied Mathematical Modelling* **36**: 139–157.

[37] Reddy J.N., 2004, *Mechanics of Laminated Composite Plates and Shells-Theory and Analysis*, CRC Press, New York.

[38] Ghorbanpour Arani A., Mosallaie Barzoki A.A., Kolahchi R., Loghman A., 2011, Pasternak foundation effect on the axial and torsional waves propagation in embedded DWCNTs using nonlocal elasticity cylindrical shell theory, *Journal of Mechanical Science and Technology* **25**: 1-8.

[39] Timoshenko SP., 1951, *Theory of Elasticity*, McGraw-Hill, New York.